Biomedicine & Pharmacotherapy 169 (2023) 115909

Contents lists available at ScienceDirect

Biomedicine & Pharmacotherapy

journal homepage: www.elsevier.com/locate/biopha

Parthenolide alleviates cognitive dysfunction and neurotoxicity via regulation of AMPK/GSK3β(Ser9)/Nrf2 signaling pathway

Jinfeng Sun [a,b,c,1], Liwei Li [b,1], Li Xiong [b], Fan Chen [b], Lingyu She [b], Hao Tang [b], Yuqing Zeng [b], Ying Duan [c], Luyao Li [b], Wei Wang [d], Gao Li [c,*], Xia Zhao [b,d,**], Guang Liang [a,b,**]

[a] Department of Pharmacy and Institute of Inflammation, Zhejiang Provincial People's Hospital, Affiliated People's Hospital, Hangzhou Medical College, Hangzhou, Zhejiang 310014, China
[b] Zhejiang TCM Key Laboratory of Pharmacology and Translational Research of Natural Products, School of Pharmaceutical Sciences, Hangzhou Medical College, Hangzhou, Zhejiang 310014, China
[c] Key Laboratory of Natural Medicines of the Changbai Mountain, Ministry of Education, College of Pharmacy, Yanbian University, Yanji, Jilin 133002, China
[d] Affiliated Yongkang First People's Hospital, Hangzhou Medical College, Hangzhou, Zhejiang 310012, China

ARTICLE INFO

Keywords:
Alzheimer's disease
Parthenolide
Cell apoptosis
Cognitive deficits
AMPK

ABSTRACT

Alzheimer's disease (AD) stands as the predominant age-related neurodegenerative disorder, for which efficacious treatment remains elusive. An auspicious avenue for this disease lies in natural compounds sourced from tranditional medicine and plant origins. Parthenolide (PTN) is a natural product with multiple biological functionsand. Recent investigations have illuminated PTN's protective properties against neurological maladies; however, its potential therapeutic role against AD remains uncharted. This study aims to explore the role of PTN in treating AD. Our *in vitro* findings underscore PTN's bioactivity, as evidenced by its capacity to curtail apoptosis, reduce reactive oxygen species (ROS) production, and restore mitochondrial membrane potential in PC12 cells. Moreover, PTN treatment demonstrates a capacity to ameliorate deficits in spatial learning and memory in the 3 ×Tg-AD murine model. Notably, PTN's therapeutic efficacy surpasses that of a clinical agent, donepezil. Mechanistically, PTN's neuroprotective effects stem from its adept regulation of the AMPK/GSK3β (ser9)/Nrf2 signaling pathway and protection on neuronal cells from ROS-related apoptosis. Although the molecular target and the pre-clinical evaluations of PTN need to be further explored, this study indicates PTN as a potential agent or lead compound for the drug development against AD.

1. Introduction

Alzheimer's disease (AD) stands as a formidable neurodegenerative disorder and represents the predominant form of dementia, regrettably bereft of efficacious pharmaceutical interventions [1]. Presently, global estimates indicate an alarming prevalence of 50 million AD cases [2]. Notably, AD pathology is fundamentally underpinned by neuronal loss, the principal driver of cognitive decline among AD patients [3]. Thus, the mitigation of neuronal apoptosis holds significant promise in impeding AD progression. The distinctive pathological hallmarks of AD encompass extracellular senile plaques (Aβ) and intracellular neurofibrillary tangles (NFTs), both potentially contributing to neuronal demise [4]. Growing evidence underscores that Aβ aggregation within the cerebral milieu precipitates mitochondrial dysfunction, excessive intracellular reactive oxygen species (ROS) generation, oxidative stress, and perturbed energy metabolism, ultimately culminating in neuronal demise through necrotic or apoptotic pathways [5,6]. Furthermore, the oxidative stress elicited by Aβ aggregation exacerbates neurotoxicity

Abbreviations: 3 ×Tg, $PS1_{M146V}/APP_{Swe}/tau_{P301L}$; Aβ, amyloid β-peptide; AD, Alzheimer's disease; AMPK, AMP-activated protein kinase; GAPDH, glyceraldehyde 3-phosphate dehydrogenase; GSK-3β, glycogen synthase kinase-3β; HO-1, heme oxygenase 1; I.P, intraperitoneal injection; MWM, Morris water maze; NFTs, neurofibrillary tangles; NOR, Novel object recognition; NQO1, NADPH, Quinone Oxidoreductase 1; Nrf2, nuclear factor erythroid-2-related factor 2; PTN, Parthenolide; ROS, reactive oxygen species; TCM, traditional Chinese medicine.

* Corresponding author.
** Corresponding authors at: Zhejiang TCM Key Laboratory of Pharmacology and Translational Research of Natural Products, School of Pharmaceutical Sciences, Hangzhou Medical College, Hangzhou, Zhejiang 310014, China.
E-mail addresses: Gaoli@ybu.edu.cn (G. Li), xiazhao@hmc.edu.cn (X. Zhao), wzmcliangguang@163.com (G. Liang).
[1] These authors contribute equally to this work.

https://doi.org/10.1016/j.biopha.2023.115909
Received 14 September 2023; Received in revised form 13 November 2023; Accepted 20 November 2023
Available online 22 November 2023

and amplifies neuronal injury [7]. Therefore, Aβ-induced oxidative stress and its ensuing apoptotic signaling cascades contribute extremely to the development of AD and may provide therapeutic strategies for this disease. AMPK emerges as a pivotal kinase for energy homeostasis regulation, wielding significant influence during AD pathogenesis, particularly in the context of Aβ deposition and oxidative stress dynamics [8,9]. Consequently, AMPK signaling and its downstream cascades have emerged as a focal point of AD research. Previous research corroborates that the interplay among AMPK, glycogen synthase kinase-3β (GSK3β), and nuclear factor erythroid-2-related factor 2 (Nrf2) signaling pathways significantly impacts anti-oxidative stress and anti-neuronal apoptosis mechanisms in AD patients [10–12]. These insights delineate novel trajectories and prospects for the development of AD therapeutics via targeting AMPK and its downstream cascade.

At present, the predominant approach in treating AD involves the use of drugs aimed at mitigating neuronal damage. Regrettably, many of the pharmaceuticals currently in use come with relatively low efficiency or associated side effects [13]. Consequently, there exists an imminent imperative to develop novel therapeutic agents for AD that are both more efficacious and safer. Medicinal plants stand out as an invaluable reservoir of unique chemical compounds characterized by intricate structures and diverse pharmacological attributes, presenting an intriguing avenue for AD drug development [14]. Within this context, we established a screening system in Aβ-challenged PC12 cells and evaluated the protective effects of our in-house natural products to find potential active compounds for alleviating AD symptoms.

In this study, we identified Parthenolide (PTN) as a potent inhibitor against $A\beta_{1-42}$-triggered apoptosis in PC12 cells from 120 in-house natural compounds. PTN has been the subject of sustained inquiry as a natural sesquiterpene lactone, known to exhibit diverse biological functionalities under pathological conditions. It serves as a secondary metabolite produced by plants of *Pyrethrum parthenium* (L.) [15]. Notably, PTN has been the subject of sustained scientific inquiry due to its multifaceted biological activities, particularly in pathological contexts. It first gained prominence for its cytotoxicity against cancer stem cells while preserving the integrity of normal cells [16]. PTN has exhibited a spectrum of remarkable pharmacological effects, spanning anticancer, antithrombotic, antiviral, hepatoprotective, and anti-inflammatory properties, and a role in neuroprotection [17,18]. However, there has been a paucity of research elucidating the role of PTN in neurodegenerative conditions such as AD. Based on our screening result, this study, for the first time, further elucidates the impact and underlying mechanisms of PTN on AD pathology both *in vitro* and *in vivo*. Our findings suggest that PTN holds promise as a potential therapeutic agent for AD prevention and treatment.

2. Materials and methods

2.1. Reagents

Parthenolide, with a purity quotient of 98.09 % (CAS: 20554–84–1), and AMPK inhibitor Compound C, with a purity quotient of 99.73 % (CAS: 1219168–18–9), were sourced from MedChemExpress, Shanghai, China. Donepezil, possessing a purity quotient of 95 % (CAS: 110119–84–1), was acquired from Chengdu Alpha Biotechnology. $A\beta_{1-42}$ (#P-2176) was purchased from Dangang Biotechnologies (Zhejiang, China). The detailed information of $A\beta_{1-42}$ is shown in the Supplementary Table S1. Reagents for cell culture, including DMEM (D1152), BSA (A8020), and FBS (F7524), were obtained from Sigma, St. Louis, MO, USA. Immunofluorescent staining (IF) reagents, such as 4,6-diamidino-2-phenylindole (DAPI; C0065), DCFH-DA reagent (S0033), and JC-1 assay (C2005), were sourced from Beyotime Biotechnology, Shanghai, China. The apoptosis detection kit (C1062L) was also procured from Beyotime Biotechnology. Hifair® V one-step RT-gDNA digestion SuperMix and SYBR Green Mix were obtained from Yeasen, Shanghai, China. A comprehensive list of antibodies utilized in this study is provided in Supplementary Table S2. The natural compounds utilized in this research were acquired from TargetMol (Boston, USA) and are listed in the Supplementary Table S3.

2.2. Cell lines and culture

Rat pheochromocytoma cells (PC12 cells, SNL-124) were procured from Sunncell Biotechnology (Wuhan, China). These cells were maintained in a culture environment comprising DMEM supplemented with 100 U/mL of penicillin-streptomycin and 10 % fetal bovine serum, within a 37 °C incubator under 5 % CO_2 conditions. The culture medium was renewed every 2 days, and cell passaging was performed at intervals of once every 3 days.

2.3. Cell viability

PC12 cells were seeded overnight in 96-well plates at a density of 1×10^4 cells per well. After achieving adherence, the cells were exposed to varying concentrations of compounds for different durations, followed by induction with $A\beta_{1-42}$ for an additional 24 h. Cells in the control group received equivalent treatment with the cell solvent. Following this 24-hour incubation, 100 μL of MTT working solution was added and incubated for 3–4 h. The MTT solution was then removed, and 100 μL of DMSO was added, followed by vigorous shaking and mixing for 10 min. The assessment of cell viability was performed by measuring absorbance at 570 nm using a microplate reader.

2.4. Detection of mitochondrial depolarization

Depolarization of mitochondrial membrane potential (ψm), an early event in the mitochondrial apoptosis cascade, was quantified using the JC-1 assay in accordance with the manufacturer's protocol, with minor adjustments as outlined in reference [19]. PC12 cells were pre-exposed to the designated concentrations of the target compounds in 96-well microplates. Subsequently, the culture supernatant was replaced with a 1 ×JC-1 solution (10 μg/mL), and the cells were incubated at 37 °C for 30–60 min. Following a thorough washing of the cells with 1 ×PBS solution twice, JC-1, selectively penetrating the mitochondria, underwent a reversible shift from a green fluorescent signal (Excitation/Emission: 485/535 nm) to a red fluorescent signal (Excitation/Emission: 488/590 nm) in response to membrane potential changes. Imaging was conducted using a fluorescence microscope equipped with a multimode microplate reader.

2.5. Reactive oxygen species (ROS) staining in cells

ROS Levels were measured using the fluorescent probe DCFH-DA reagent, following the manufacturer's protocol. In brief, PC12 cells were pre-exposed to the appropriate compounds, as previously outlined, and subsequently incubated in a serum-free medium supplemented with 10 mM DCFH-DA for 30–60 min. Following this incubation, cells were subjected to two washes with PBS solution. Untreated cells served as the negative control. Subsequently, we quantified the fluorescence intensity in each well using an Infinite M200 PRO microplate reader with excitation and emission wavelengths set at 488 nm/525 nm [20]. The green fluorescence intensity was directly proportional to the intracellular ROS levels.

2.6. Apoptosis detection by flow cytometry

PC12 cells were initially seeded in a 12-well plate at a density of 5×10^5 cells per well and cultured for 24 h. Subsequently, the cells were subjected to pretreatment with the designated target compounds, as previously described [4]. The analysis was carried out through flow cytometry in accordance with the instructions provided by the supplier, employing the Annexin-VFITC/PI apoptosis detection kit. The cells were

then resuspended in a 1 ×binding buffer and incubated at room temperature in the dark for 40 min with 5 μL of FITC-labeled annexin V. Subsequently, 5 μL of propidium iodide staining was introduced, and under the same conditions, incubation was allowed to proceed for an additional 5 min. The flow cytometry analysis was conducted using the BD Accuri C6 Plus instrument (Biosciences, USA) to detect both late and early apoptotic cells. Data analysis was performed using Flow Jo V10.0 software.

2.7. Real-time quantitative PCR

To assess the impact of PTN on mRNA transcripts of cytokines, we conducted quantitative real-time polymerase chain reaction (qRT-PCR) analyses. RNA was extracted from the cells using Trizol Reagent and subsequently converted into complementary DNA (cDNA) following the manufacturer's protocols, utilizing the Hifair® V one-step RT-gDNA digestion SuperMix. The amplification of the target transcripts was accomplished using SYBR Green Mix in a CFX Connect real-time PCR system (Bio-Rad). The primer sequences corresponding to the genes of interest were synthesized and sourced from Thermo Fisher. The primers employed in this study are listed in the Supplementary Table S4.

2.8. Animal and treatment

For our investigations, we employed the 3 ×Tg-AD mouse model of Alzheimer's disease, characterized by the presence of three human mutant alleles, specifically harboring PS1M146V knockin, APPswe and TauP301L transgenes. These mice (10 months, 28–30 g, female) were procured as breeding pairs from the Jackson Laboratories and were bred in the animal facility at Hangzhou Medical College. This model exhibits age-related cognitive decline and displays pathological features including extracellular amyloid plaques and tau pathology. The mice were housed in a group within a tranquil facility, under conditions of a 12-hour light and dark cycle, with room temperatures maintained between 20 and 24 ℃. They were provided ad libitum access to both food and water. All experimental procedures strictly adhered to the guidelines outlined in the National Institutes of Health Guide for the Care and Use of Laboratory Animals. Additionally, these procedures received approval from the Hangzhou Medical College Animal Ethics Committee. Random allocation resulted in the division of the mice into five groups, each comprising 10 individuals: Wild-type (WT), 3 ×Tg, 3 ×Tg+ 1 mg/kg PTN, 3 ×Tg+ 5 mg/kg PTN, and 3 ×Tg+ 5 mg/kg donepezil [21]. All drugs were dissolved in 2 % DMSO in PBS, and the control group was given an equal volume of 1xPBS (containing 2 % DMSO). All groups were injected intraperitoneally once a day for one month.

Throughout the experiment, all mice exhibited survival. Upon completion of the experimental protocol, euthanasia was carried out using injectable pentobarbital sodium. Brain tissue from the mice was harvested and promptly frozen in liquid nitrogen for subsequent protein expression analysis, while 4 % paraformaldehyde (PFA) treatment was utilized for histological examination.

2.9. The Morris Water Maze (MWM)

The MWM represents a widely utilized test paradigm for the assessment of spatial learning abilities in rodents [22]. In our investigation, we subjected mice to the MWM test, employing a methodology consistent with our previous studies, to evaluate the impact of PTN on spatial memory and learning capabilities. The experimental setup and procedures in this study remained in line with our prior research endeavors [23]. Preceding the commencement of the experiment, mice underwent a three-day training period during which they familiarized themselves with locating the hidden platforms. The time taken to find the platform, referred to as latency, was recorded during the training sessions. On the fifth day, the platform was removed, and the mice were subjected to two trials during which they were allowed unrestricted movement for 60 s within two quadrants, neither of which contained the platform. These trials were meticulously monitored and analyzed using a recording system (VisuTrack, Shanghai, China), which tracked parameters such as platform crossings and the time spent within the target quadrant.

2.10. Novel object recognition (NOR)

The NOR task represents a widely employed behavioral assay for the assessment of episodic-like declarative memory in rodents, capitalizing on their inherent proclivity for exploring novelty [24]. During the initial training session, mice were positioned within the confines of an open cube test box (50 ×50 ×50 cm^3) and allowed to freely explore two identical objects, denoted as Object A, for 5 min. Exploratory behavior encompassed instances where the mice made physical contact with the objects or probed them within a proximity of 2–3 cm. On the subsequent day, Object A was substituted with a novel object, Object B, and the mice were afforded a 5-minute window for unimpeded exploration. All trials were meticulously recorded employing NOR equipment.

2.11. Western blotting analysis

Total protein was extracted from both mouse tissue and cell culture specimens using RIPA buffer, which was supplemented with a protease and phosphatase inhibitor cocktail. To ascertain protein concentrations, a BCA protein assay kit was employed, and an equivalent quantity of protein was loaded and subsequently subjected to separation via sodium dodecyl sulfate-polyacrylamide gel electrophoresis (SDS-PAGE). The separated proteins were subsequently transferred onto polyvinylidene fluoride (PVDF) membranes, and then which were incubated with protein-free rapid blocking buffer for 30 min at room temperature. Following this blocking procedure, the PVDF membranes underwent an overnight incubation at 4 ℃ with specific primary antibodies. The subsequent day, the membranes were subjected to three consecutive washes, followed by an incubation step at room temperature lasting 1–2 h with the appropriate HRP-conjugated secondary antibodies. Finally, the blots were imaged utilizing an enhanced chemiluminescence (ECL) reagent, and quantitative analysis was performed using Image J software.

2.12. Immunofluorescent staining (IF)

Brains from each experimental group were subjected to fixation in 4 % PFA at 4 °C for 8–12 h. Following fixation, a sucrose gradient was utilized for dehydration, and the brains were subsequently embedded in an optimized cutting temperature compound (OCT). Serial cryostat sections, each with a thickness of 25 μm and targeting the hippocampal region, were obtained. These sections were subjected to blocking using 10 % BSA for 60 min at 37 °C, and then incubated at 4 °C with primary antibodies, after which they were exposed to the appropriate Alexa-Fluor-conjugated secondary antibodies for 2 h at 37 °C. Nuclei were counterstained using DAPI, which included an anti-fluorescence quencher. Ultimately, the sections were examined utilizing a Nikon A1 laser confocal microscope (Nikon, Japan) and subsequent analysis was carried out employing ImageJ software.

2.13. Statistical analysis

Statistical analysis to assess the significance of observed differences among various groups was conducted employing GraphPad Prism 8 software. All experiments were executed in triplicate, and the resulting data was presented as the mean ± standard error of the mean (SEM). To ascertain statistical disparities between groups, either two-way or one-way analysis of variance (ANOVA) was applied, followed by Tukey's post-hoc test, with a significance level (α) set at 0.05.

3. Results

3.1. PTN prevents Aβ-induced injury in PC-12 cells

Recent reports have indicated that neurotoxicity induced by Aβ primarily manifests through apoptosis, mitochondrial dysfunction, and oxidative stress mechanisms, especially $A\beta_{1-42}$ [25]. In pursuit of evaluating the anti-apoptotic potential of a in-house bank of 120 natural compounds (Supplementary Table S3), we conducted an MTT assay in PC12 cells challenged with $A\beta_{1-42}$ at 10 μM. Remarkably, our findings revealed that PTN (at 10 μM) exhibited the most pronounced protective effect against $A\beta_{1-42}$-induced neuronal cell death (Fig. 1A-B). Furthermore, our investigation demonstrated that PTN, within the concentration range of 1–20 μM, exerted minimal cytotoxicity on PC12 cells (as depicted in Fig. S1). Intriguingly, PTN exhibited a concentration-dependent restoration of the viability of $A\beta_{1-42}$-stimulated PC12 cells, as illustrated in Fig. 1C. In light of the previous publications, PTN has showed robust antioxidative effects in other diseases [26,27]. Subsequent analyses revealed that PTN significantly attenuated oxidative stress and reinstated mitochondrial membrane potential (Fig. 1D, F, G). To further substantiate the protective effects of PTN against apoptosis, flow cytometry data demonstrated a marked reduction in apoptotic cells compared to the $A\beta_{1-42}$-exposed group (Fig. 1E, H). Moreover, we conducted an assessment of apoptosis through both western blot analysis and mRNA levels. The results revealed that following the stimulation of PC12 cells by $A\beta_{1-42}$, there was a notable upregulation in Bax and cleaved-caspase 3 levels, concomitant with a decrease in Bcl2 levels. Notably, these alterations were effectively mitigated by PTN pretreatment in a dose-dependent manner (Fig. 1I-K). Thus, PTN emerged as a potent agent in mitigating $A\beta_{1-42}$-induced injury responses in PC-12 cells.

3.2. PTN protects PC12 cells via regulation of AMPK/GSK3β(Ser9)/Nrf2 signaling pathway

We proceeded to explore the mechanisms underlying PTN's antioxidative and anti-apotosis activity in $A\beta_{1-42}$-induced cells. Based on the significant role of AMPK/GSK3β(Ser9)/Nrf2 signaling pathway in mediating ROS-related neuronal injuires, we examined whether PTN treatment could orchestrate regulation of this signaling pathway in PC12 cells. Interestingly, western blot analyses unveiled that the $A\beta_{1-42}$ group exhibited diminished phosphorylation of AMPK and GSK3β(Ser9), coupled with suppressed Nrf2 expression. Conversely, PTN pretreatment robustly reinstated these effects (Fig. 2A-B). As shown in the Supplementary Fig. S3, PTN treatment also significantly increased the nuclear localization of Nrf2 in $A\beta_{1-42}$-challenged PC12 cells. Nrf2 regulates the expression of key antioxidant genes such as NAD(P)H: quinone oxidoreductase 1 (NQO1) and heme oxygenase 1 (HO-1) [28]. PTN also significantly upregulated the mRNA levels of *Nrf2, NQO1* and *HO-1* in $A\beta_{1-42}$-induced cells (Fig. 2C). To ascertain the role of AMPK in mediating PTN's antioxidative stress effects, we employed Compound C (dorsomorphin), a well-established AMPK inhibitor. Western blotting analyse indicated that Compound C treatment reversed the inhibitory effect of PTN on $A\beta_{1-42}$-induced PC12 cell apoptosis, as well as a dampening of PTN's activation of the AMPK/GSK3β(Ser9)/Nrf2 signaling pathway (Fig. 2D-F). As expected, AMPK inhibitor compound C also reversed PTN-increased nuclear level of Nrf2 (supplementary Fig. S4). JC-1 and ROS stainings further confirmed that Compound C pretreatment negated PTN's protective effect against oxidative stress (Fig. 2G, I, J). Moreover, PTN-reduced apoptosis in $A\beta_{1-42}$-challenged PC12 cells was also reversed by Compound C treatment (Fig. 2H, K). These findings collectively suggest that PTN effectively promotes neuroprotection in PC12 cells by orchestrating the regulation of the AMPK/GSK3β(Ser9)/Nrf2 signaling pathway.

3.3. PTN improved the cognitive impairment of 3 ×Tg-AD mice

We employed a triple transgenic murine model for AD (3 ×Tg-AD mice), which is widely acknowledged for its inclusion of both Aβ and tau pathologies and closely mimics the characteristics of the human disease. We selected female 3 ×Tg-AD mice for our study due to their known rapid progression of AD pathology compared to males [29]. The optimization of dosage, treatment duration, and administration route of PTN was based on established PTN administration studies [18] and the experimental design of MWM as depicted in Fig. 3A. Motion tracks of the mice during the probe trial and place navigation test of the MWM are illustrated in Fig. 3B. Notably, our analysis did not reveal any significant differences in the total distance covered and mean swimming speed across all test groups during posthoc multiple comparisons (Fig. 3C-D). This substantiates the MWM results as a reliable indicator of PTN's impact on memory impairment in 3 ×Tg-AD mice. Furthermore, based on the results of the place navigation test, PTN treatment notably resulted in a significant increase in the time spent within the target quadrant and an elevated number of platform crossings. Importantly, PTN's therapeutic effect surpassed that of the clinical control drug, donepezil (Fig. 3E-F). To gauge spatial learning abilities, we analyzed the time each mouse required to locate the hidden platform in the MWM, with escape latency being inversely correlated with spatial learning proficiency. Analysis of the escape latency and distance covered within the target quadrant revealed that, in comparison to WT mice, 3 ×Tg-AD mice exhibited significantly prolonged escape latency and reduced distance within the target quadrant during platform location. However, PTN-treated animals exhibited noteworthy improvements in cognitive function. Notably, the high-dose PTN treatment group outperformed the donepezil group in terms of escape latency and distance within the target quadrant (Fig. 3G-H). These findings strongly suggest that PTN holds the potential to ameliorate the learning and memory deficits in the 3 ×Tg-AD mouse model.

The NOR test was employed to assess the impact of PTN on the memory capacity of rodents, capitalizing on rodents' inherent inclination to approach and explore novel objects. As illustrated in Fig. 4A, we present the motion trails and heat maps of mice across various experimental groups (Fig. 4B). As anticipated, the initial exploration tendencies of the 3 ×Tg-AD mice group exhibited a reduced inclination compared to the WT group. However, this propensity for exploration markedly improved following the administration of treatment (Fig. 4C-D). Upon the introduction of a novel object on the subsequent day, the PTN-treated group exhibited a distinct preference for the novel object. Remarkably, this effect surpassed that observed in the donepezil group. In contrast, the 3 ×Tg-AD group demonstrated a diminished ability to recognize the new object, with an equal amount of time spent exploring both familiar and novel objects (Fig. 4E). These findings collectively reinforce the notion that PTN substantially enhances the cognitive capacity of 3 ×Tg-AD mice.

3.4. PTN treatment reduced AD pathology in the hippocampus of 3 ×Tg-AD mice

To investigate whether PTN confers beneficial effects in mitigating Aβ pathology, we conducted immunofluorescence analyses to assess the expression of key markers, including APP/β-amyloid, GFAP (an astrocytic marker), and Iba1 (a microglial marker). As anticipated, the levels of these markers were significantly elevated in the model mice compared to the WT group. Remarkably, treatment with PTN led to a substantial reduction in Aβ plaque density, as well as in the numbers of GFAP-positive and Iba1-positive cells (Fig. 5A-D). Additionally, we quantified their expression levels through western blotting in brain tissue samples. As depicted in Fig. 5E-F, protein expression within the hippocampus of 3 ×Tg-AD mice exhibited significant increases. However, these elevated levels were nearly completely reversed in mice treated with PTN, akin to the outcomes observed in the donepezil group.

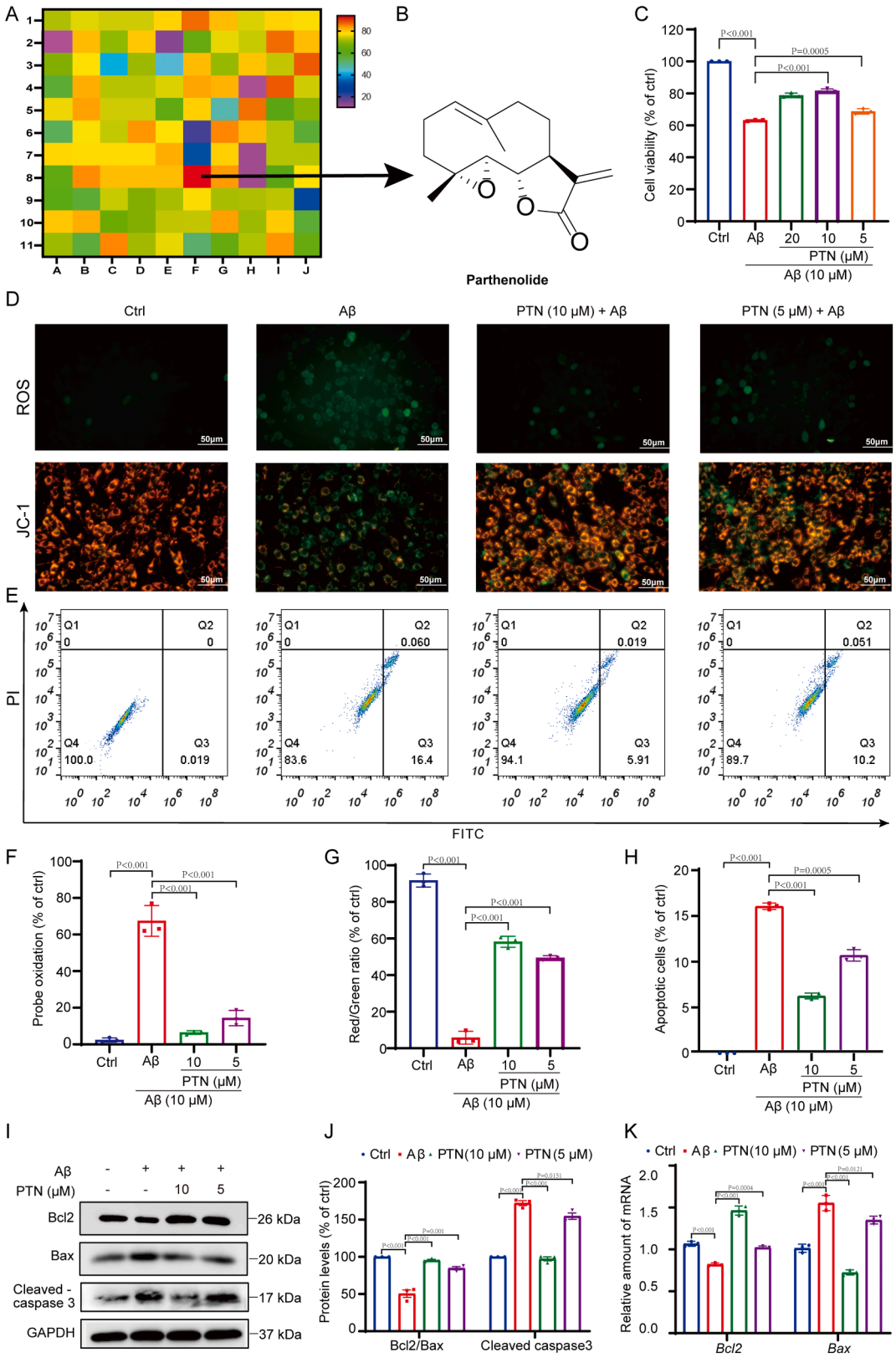

Fig. 1. PTN decreased $A\beta_{1-42}$-induced apoptosis in PC12 Cells. (a) Cell viability was measured by MTT assay after pretreatment of 120 natural compounds at 10 mM for 2 h in PC12 cells, respectively, and then induced with or without 10 μM $A\beta_{1-42}$ for a further 24 h. (B) Chemical structure of Parthenolide (PTN). (C) MTT assay was performed on PC12 cells to determine the viability of PTN. (D) As assessing intracellular ROS levels with ROS staining, and JC-1 staining was used for △ψm. (E) Flow cytometry was used to determine apoptosis. (F) The percentage with quantitative analysis of ROS levels. (G) Fluorescence intensity ratio of red to green (an increase in mitochondrial membrane potential). (H) Quantitative data of apoptotic cells in E. (I-J) GAPDH was used as a loading control in this western blot analysis of Bax, cleaved-caspase 3, and Bcl2 in PC12 cells. Image J software in plane A was used to determine the quantitative intensity of the blots of these proteins. (K) In the PC12 cells, the mRNA levels of *Bax* and *Bcl2* were detected via RT-qPCR. All quantitative data are presented as mean ± SEM (n = 3).

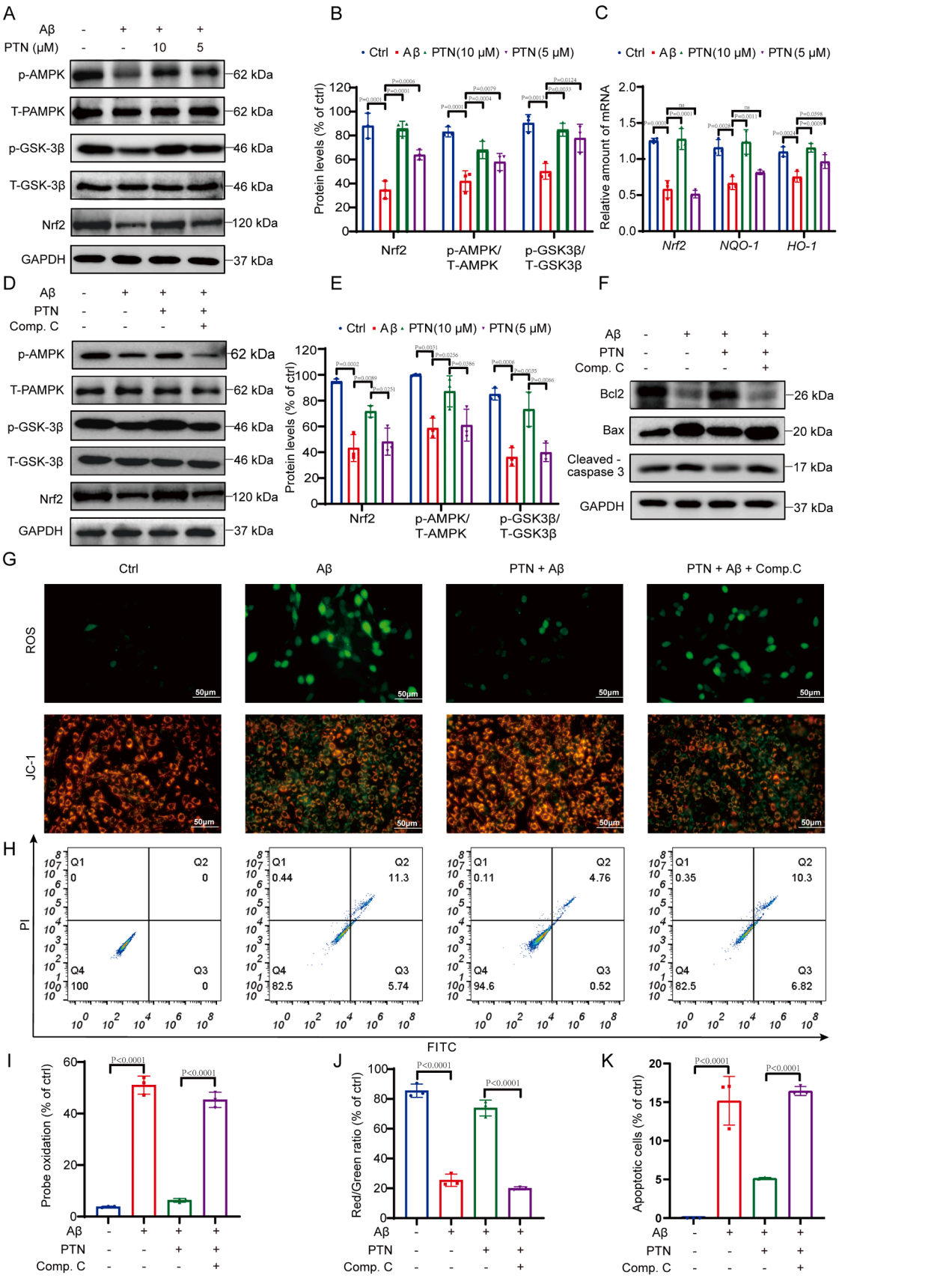

(caption on next page)

Fig. 2. PTN conferred neuroprotection via regulation of AMPK/GSK3β(Ser9)/Nrf2 signaling pathway in PC12 cells. Pretreatment of PC12 cells with 10 μM or 5 μM PTN for 2 h followed by exposure for 24 h with 10 μM $A\beta_{1-42}$ in PC12 cells. (A-B) GAPDH was used as the loading control, p-AMPK, T-AMPK, p-GSK-3β, T-GSK-3β, and Nrf2 were the representative western blot analysis, and the quantitative data of the blot intensity determined by Image J software in plane A. (C) mRNA levels of *Nrf2, NQO-1,* and *HO-1* were detected via quantitative RT-qPCR in PC12 cells. (D-I) PC12 cells were pretreated with or without 2 μM compound C. (D-E) Western blot to test the expression of p-AMPK, T-AMPK, p-GSK-3β, T-GSK-3β, and Nrf2 in PC12 cells after AMPK inhibitor. Image J software in plane A was used to determine the quantitative intensity of the blots of these proteins. (F) Western blot analysis results of representative apoptosis-related protein (Bax, Cleaved-caspase 3, and Bcl2) in PC12 cells after AMPK inhibitor. (G) After AMPK inhibitor, ROS levels with ROS staining, MMP with JC-1 staining. (H) Cell apoptosis after the AMPK inhibitor was measured by flow cytometry. (I) Quantitative analysis of percentages of the cellular ROS level after AMPK inhibitor. (J) Fluorescence intensity ratio of red to green after AMPK inhibitor. (K) Quantitation of the percentage of cell apoptosis after AMPK inhibitor. Results are presented as mean ± SEM (n = 3). ns = not significant.

3.5. PTN decreased neuronal apoptosis in the hippocampus of 3 ×Tg-AD mice by activation of the AMPK/GSK3β(Ser9)/Nrf2 signaling pathway

Hippocampal neuronal damage has been established as the primary underlying factor contributing to cognitive impairment in AD. The anatomical depiction of the hippocampal formation is illustrated in Fig. 6A. Notably, a substantial increase in NeuN-positive cells was observed following treatment with PTN or donepezil, as depicted in Fig. 6B-C. Furthermore, we conducted western blotting to examine the expression levels of proteins associated with apoptosis in hippocampal tissue. In harmony with our cellular findings, PTN treatment led to a remarkable increase in the Bcl-2/Bax expression ratio, along with a reduction in cleaved caspase-3 expression. This observed effect closely mirrored the outcomes observed in the donepezil treatment group (Fig. 6D-E). Our final objective encompassed an assessment of the neuroprotective potential of PTN, with a particular focus on its influence on the AMPK/GSK3β(Ser9)/Nrf2 signaling pathway within hippocampal tissue, employing western blot analysis. These findings unveiled that PTN treatment induced a significant upregulation in the expression levels of phosphorylated AMPK (p-AMPK), phosphorylated GSK-3β (p-GSK-3β), and Nrf2 when compared to the WT group (Fig. 6F-G). In summation, PTN exhibited a pronounced capacity to suppress apoptosis and mitigate oxidative stress, a phenomenon attributed to its ability to enhance the activation of the AMPK/GSK3β(Ser9)/Nrf2 signaling pathway in AD.

4. Discussion

In this investigation, we elucidate that PTN exerts a significant ameliorative effect on $A\beta_{1-42}$-induced PC12 cell apoptosis by reinstating mitochondrial membrane potential and reducing intracellular ROS levels. Furthermore, our mechanistic inquiries reveals that PTN protects neuronal cells via activating AMPK/GSK3β(Ser9)/Nrf2 signaling pathway. The anti-ROS and anti-apoptosis activities of PTN were counteracted upon the inhibition of AMPK by Compound C. *In vivo*, PTN treatment effectively alleviated cognitive deficits and pathological hallmarks in 3 ×Tg-AD mice. These therapeutic benefits were notably associated with the activation of the AMPK/GSK3β(Ser9)/Nrf2 signaling pathway. Importantly, PTN treatment demonstrated superior therapeutic efficacy compared to donepezil. Collectively, our data present PTN as a potential candidate or a lead compound in the pursuit of therapeutics for AD.

Currently, the therapeutic landscape for AD remains limited, with only five approved medical interventions available, all of which are primarily geared towards symptom management rather than altering the disease's trajectory [30]. The recent approval by the US Food and Drug Administration of aducanumab, an antibody targeting Aβ, marked a notable milestone as the first Alzheimer's drug endorsement in nearly two decades. However, concerns regarding undesired side effects have cast a shadow over the landscape of AD therapeutics [31]. The exploration of natural products emerges as a promising avenue for drug discovery. Natural products offer a vast reservoir of chemical diversity, diverse biological activities, and a range of molecular properties that render them invaluable for uncovering novel therapeutic agents [32]. Here, we first provided a pioneering effort to demonstrate the anti-oxidative and anti-apoptosis efficacy of PTN, which contributed to safeguarding neuronal integrity and improved memory deficits in AD mice.

PTN, a prominent sesquiterpene lactone, has garnered attention for its recognized potential in the realms of anti-oxidative, anti-inflammation, and anti-cancer activity [33]. Previously, PTN had a therapeutic potential as an antitumor agent for glioblastoma and can cross the blood–brain barrier [34,35]. In this context, our evidences lend credit to the new discovery of a repurposing role for PTN against AD with the mechanism through reduing oxidative stress and mitochondrial dysfunction. It is noted that chronic inflammation, including the activation of glial cells and the release of inflammatory mediators, represents another crucial role in AD pathology [36]. In this aspect, a lot of previous studies have demonstrated that PTN showed anti-inflammatory activities in other diseases [33]. Therefore, in addition to the regulation of AMPK/GSK3β(Ser9)/Nrf2-ROS pathway, the anti-inflammatory actions of PTN may also contribute to the alleviation of AD pathology. The potential involvement of anti-inflammatory mechanism in PTN treatment against AD is interesting and deserve further research. In addition, PTN has low solubility and bioavailability, limiting its *in vivo* application. ACT001 is derived and synthesized from PTN, currently undergoing Phase II clinical trials for the treatment of Glioblastoma, which retains the advantageous properties of PTN while featuring improved stability, solubility, low toxicity, and minimal side effects [37]. Our results also suggest that it is valuable to evaluate the therapeutic effects of ACT001 on AD, which may provide a new and important application for ACT001 development.

The cascade of events involving mitochondrial respiratory chain disruption and the initiation of neuronal apoptosis due to oxidative stress stands as a pivotal precursor in the pathogenesis of AD. Therefore, the natural products with promising antioxidant activity may serve as therapeutic candidates to treat AD [38]. PTN demonstrates robust antioxidative properties. Furthermore, PTN enhances the activity of antioxidant enzymes, and induces the mRNA expression of *Nrf2*, *HO-1*, and *NQO1* [39]. The evidence underscores that natural antioxidants possess the capacity to mitigate Aβ-induced neurotoxicity [40]. Considering this accumulating evidences, therapeutic potential of PTN against AD have been keenly focused on reducing oxidative stress and mitigating mitochondrial impairment, thereby inhibiting the apoptotic cascade.

AMPK, known for its significant influence on oxidative stress and mitochondrial function modulation, assumes paramount importance in AD pathology. Prolonged oxidative stress in AD is characterized by the inhibition of GSK-3β(ser9) activation, a concurrent downregulation of Nrf2 and its downstream target genes, such as *NQO-1* and *HO-1*. This cumulative effect curtails the cellular antioxidant capacity and promotes cellular demise [41]. Furthermore, GSK3β and Nrf2 acting as the key downstream target of AMPK has garnered attention for its potential role in enhancing cortical neuroprotection. Metformin substantiates its neuroprotective efficacy through the modulation of the AMPK/mTOR signaling pathway, primarily by inhibiting tau phosphorylation [42]. Several natural antioxidants have garnered increasing attention for their potential in the prevention and treatment of AD via regulating AMPK signaling pathway. Notably, Li et al. have illuminated the neuroprotective attributes of artemether against Aβ-induced neurotoxicity, with concurrent activation of the AMPK/GSK3β(ser9)/Nrf2 signaling cascade [43]. The polyphenol resveratrol enhances mitochondrial

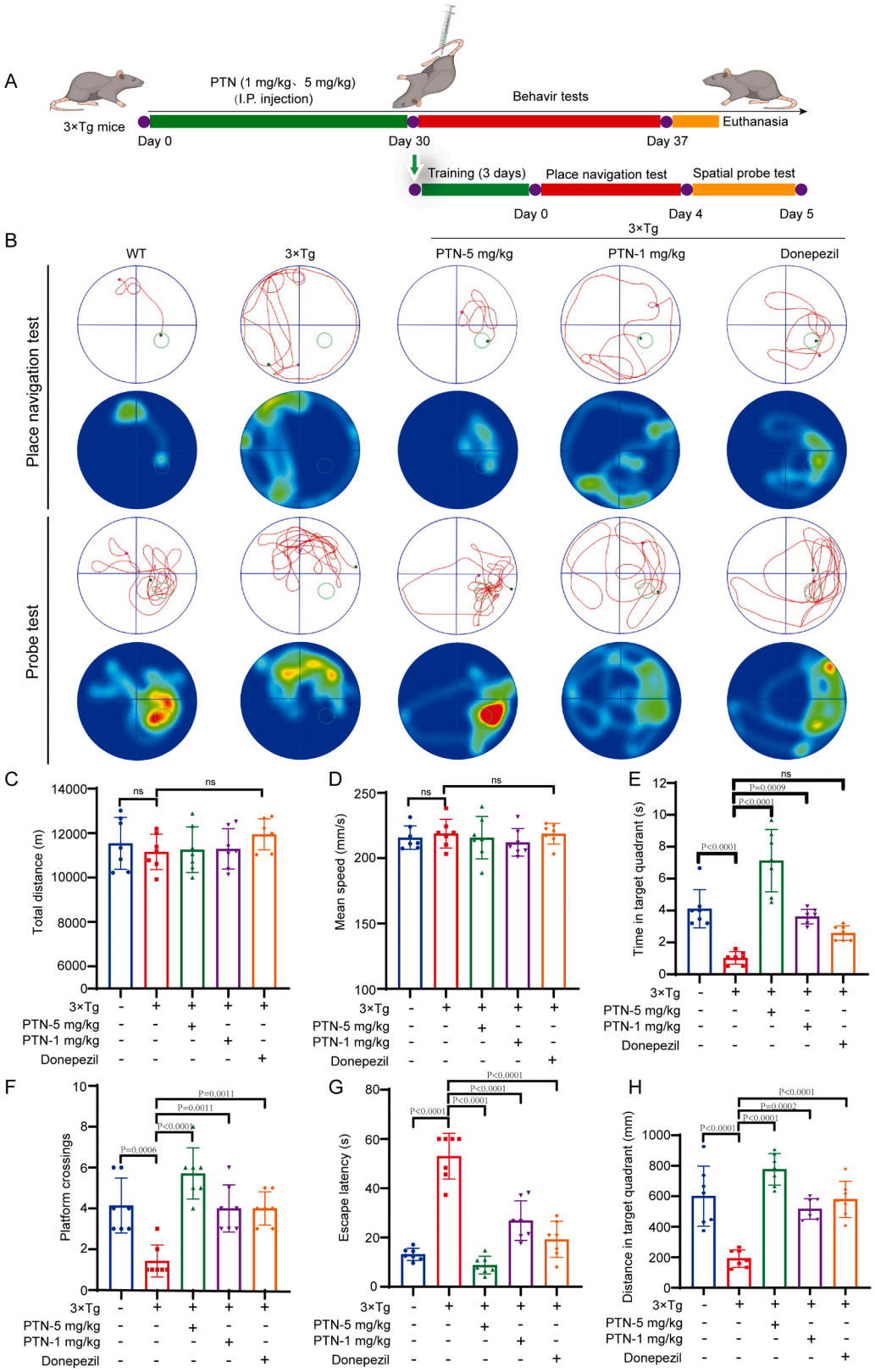

Fig. 3. PTN improved learning and memory deficits in 3 ×Tg-AD mice. (A) The timeline of 10-month-old 3 ×Tg-AD mice was pretreatment of PTN injections were administered intraperitoneally every day for a month and behavioral tests were conducted. (B) The representative swimming trace of place navigation test and probe test in MWM. (C) Total distance of mice. (D) Mean swimming speed of mice. (E) During the training trails, The time of escape latency to the platform in a MWM. (F) Probe test with the time spent in the target quadrant. (G) On the fifth day, the mice of each group crossed platforms within 60 s (H) The distance in target quadrant. Data are presented as mean ± SEM, n = 7. ns = not significant.

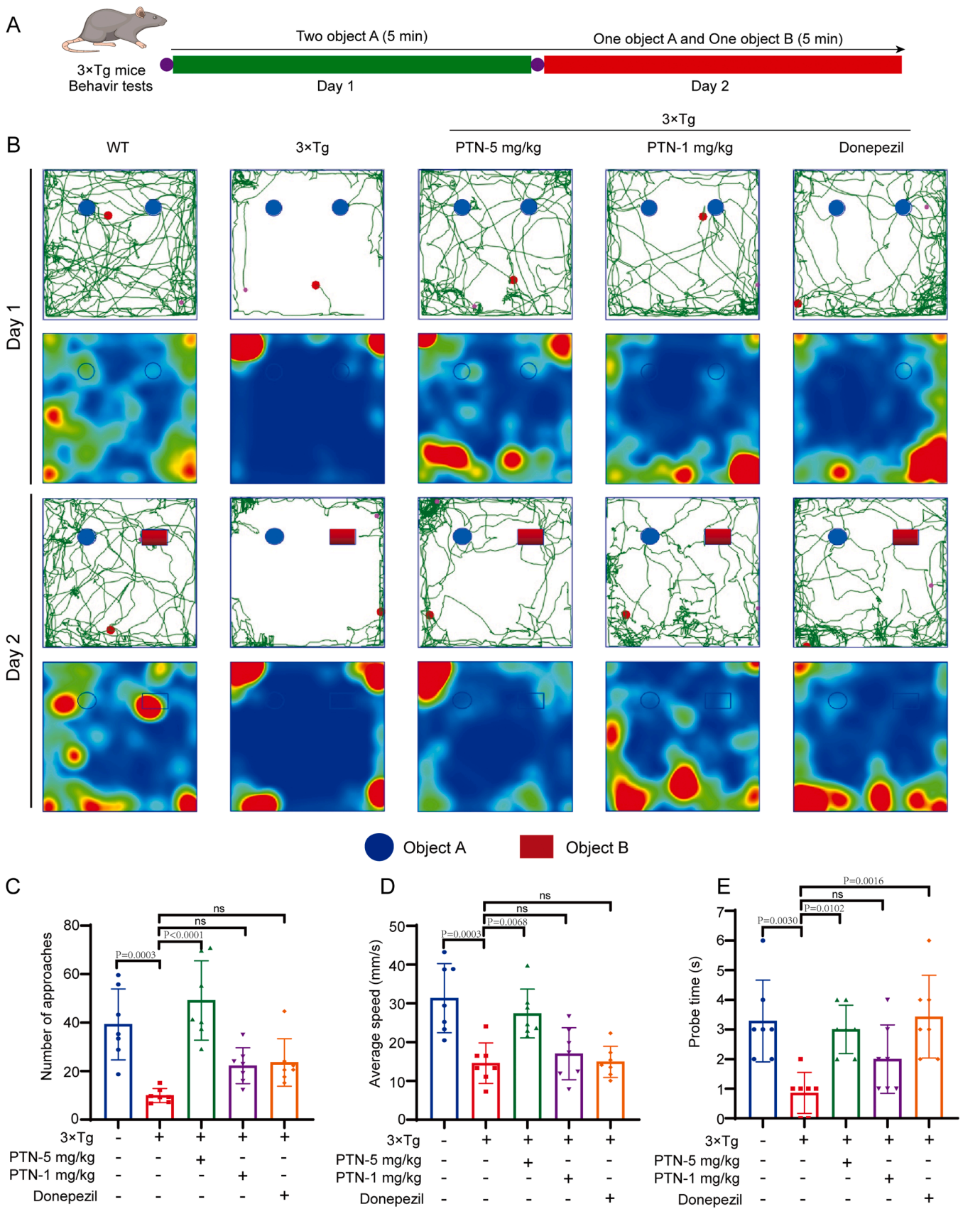

Fig. 4. PTN alleviates the cognitive impairment in 3 ×Tg-AD mice. Timeline of NOR test. (B) Representative images for NOR experiment. (C-D) On the second day, the number of approaches for novel objects and the average speed. (E) The probe time of the novel object approaches on the second day. Data are presented as mean ± SEM, n = 7. ns = not significant.

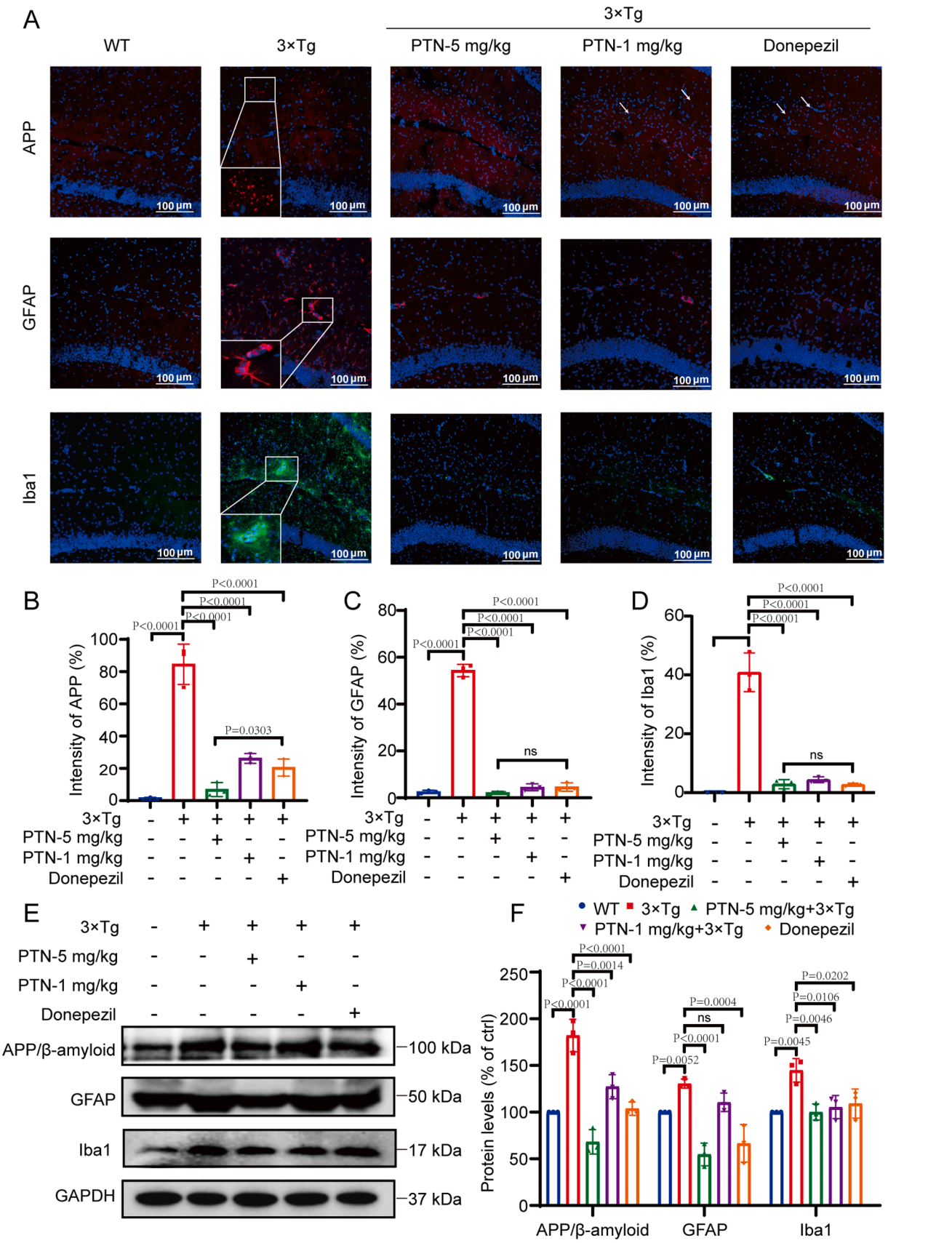

Fig. 5. PTN treatment reduced AD pathology of 3 ×Tg-AD mice. APP/β-amyloid, GFAP, and Iba1 immunofluorescence images of the hippocampus (scale bar is 100 μm). (B-D) Fluorescence quantification of APP/β-amyloid, GFAP, and Iba1. (E) GAPDH was used as the loading control. Western blot to test the expression of APP/β-amyloid, GFAP, and Iba1 in the hippocampus. (F) Image J software in plane A was used to determine the quantitative intensity of the blots of these proteins. Data are presented as mean ± SEM, n = 7. ns = not significant.

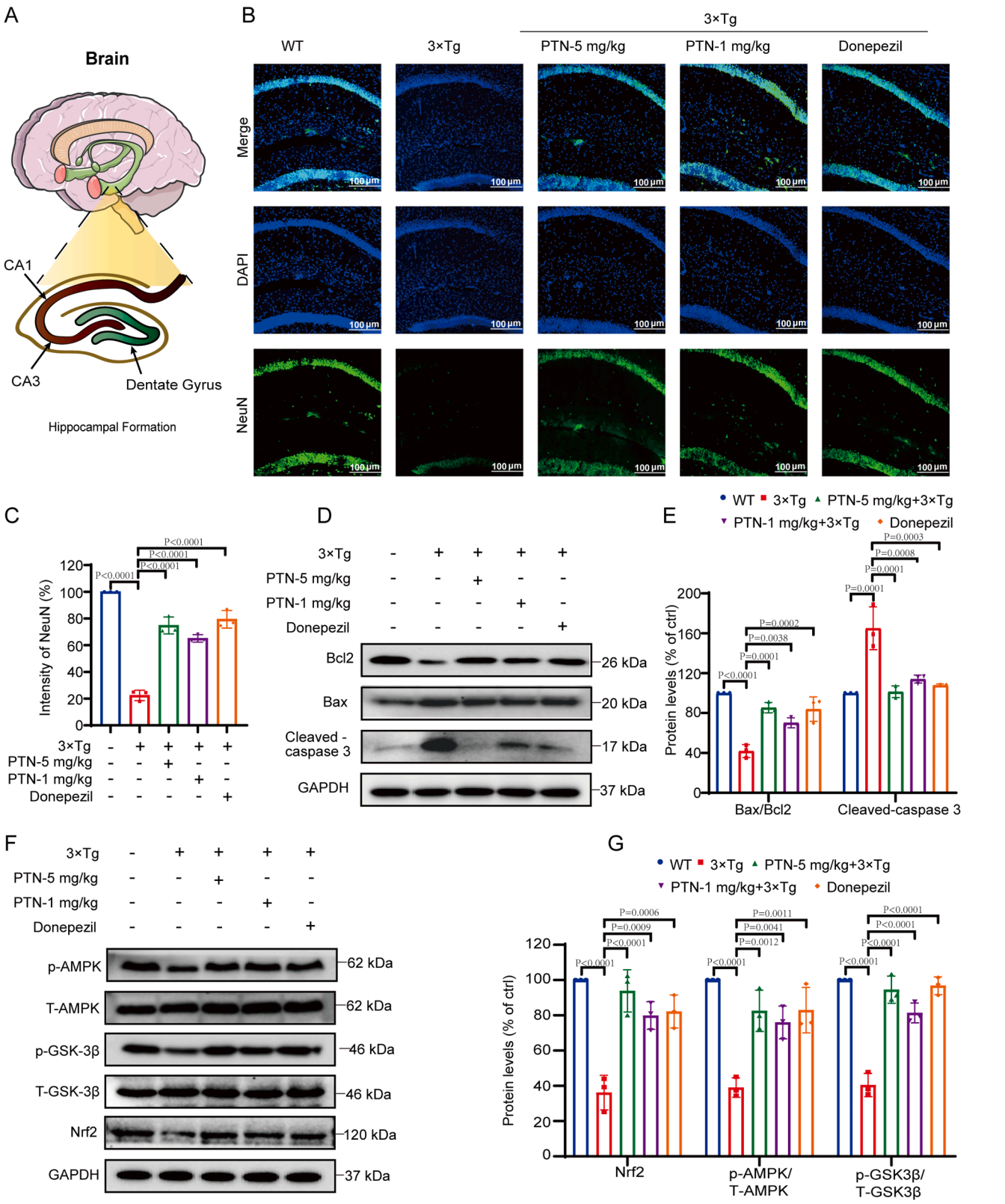

Fig. 6. PTN treatment decreased neuronal apoptosis in the hippocampus of 3 ×Tg-AD mice by activation of the AMPK/GSK3β(Ser9)/Nrf2 signaling pathway. Hippocampal formation. (B) NeuN immunofluorescence of the hippocampus. (C) Fluorescence quantification of NeuN. (D) Western blot analysis results of representative apoptosis-related protein (Bax, Cleaved-caspase 3 and Bcl2). GAPDH was used as the loading control. (E) Quantitative data of the apoptosis-related proteins by Image J software. (F-G) Representative western blot analysis of p-AMPK, T-AMPK, p-GSK-3β, T-GSK-3β, and Nrf2 in the hippocampus and Image J software was used for the analysis of quantitative data of the blot intensity. Data are presented as mean ± SEM, n = 7.

energetic function, and improves Aβ-peptide clearance by activating SIRT1 and AMPK [44]. In addition, our investigation has documented the neuroprotective impact of Ginsenoside Rk3, associated with AMPK activation [23]. In this study, we unveil a novel facet of PTN action, wherein it modulates the AMPK/GSK3β(ser9)/Nrf2 signaling pathway, offering new prospects for the treatment of AD.

In summary, our investigation has unveiled the neuroprotective attributes of PTN, elucidating its capacity to mitigate oxidative stress and, consequently, suppress the apoptotic cascade. This effect is achieved through the modulation of the AMPK/GSK3β(ser9)/Nrf2 signaling pathway, both in *in vivo* and *in vitro* settings. Although the molecular target and the pre-clinical evaluations of PTN need to be further explored, PTN emerges as a compelling candidate or lead compound for prospective therapeutic interventions targeting AD treatment.

CRediT authorship contribution statement

Guang Liang, Xia Zhao and **Gao Li** were responsible for conceptualizing and designing the core research framework and played a pivotal role in data analysis. **Jinfeng Sun** took the lead in drafting the initial manuscript. **Jinfeng Sun, Liwei Li, Li Xiong, Lingyu She, Hao Tang**, and **Yuqing Zeng** conducted the experimental procedures. **Gao Li, Fan Chen**, and **Xia Zhao** were instrumental in revising and enhancing the manuscript. **Hao Tang, Liwei Li, Yuqing Zeng, Li Xiong, Ying Duan**, and **Luyao Li** were actively involved in data acquisition and its subsequent analysis.

All authors have read and approved the final manuscript. All authors contributed to data analysis, drafting or revising the article, agreed on the journal to which the article will be submitted, gave final approval of the version to be published, and agreed to be accountable for all aspects of the work.

Declaration of Competing Interest

The authors have no conflicts of interest to declare.

Data availability

Data will be made available on request.

Acknowledgements

This study was supported by the National Natural Science Foundation of China (82360805 to J.F.S.), Zhejiang Provincial Key Scientific Project (2021C03041 to G.L.), Natural Science Foundation of Zhejiang Province (LQ23H090018 to X.Z.) and Hangzhou Medical College (00004F1RCYJ2109 to X.Z.).

Appendix A. Supporting information

Supplementary data associated with this article can be found in the online version at doi:10.1016/j.biopha.2023.115909.

References

[1] Y. Zhao, D. Hu, R. Wang, X. Sun, P. Ropelewski, Z. Hubler, K. Lundberg, Q. Wang, D.J. Adams, R. Xu, X. Qi, ATAD3A oligomerization promotes neuropathology and cognitive deficits in Alzheimer's disease models, Nat. Commun. 13 (2022), 1121, https://doi.org/10.1038/s41467-022-28769-9.

[2] A. Gustavsson, N. Norton, T. Fast, L. Frölich, J. Georges, D. Holzapfel, T. Kirabali, P. Krolak-Salmon, P.M. Rossini, M.T. Ferretti, L. Lanman, A.S. Chadha, W.M. Van Der Flier, Global estimates on the number of persons across the Alzheimer's disease continuum, Alzheimers Dement. 19 (2023) 658–670, https://doi.org/10.1002/alz.12694.

[3] 2023 Alzheimer's disease facts and figures, Alzheimers Dement. 19 (2023) 1598–1695, https://doi.org/10.1002/alz.13016.

[4] L. Zhong, Y. Qin, M. Liu, J. Sun, H. Tang, Y. Zeng, J. Zhang, W. Wang, G. Liang, X. Zhao, Magnoflorine improves cognitive deficits and pathology of Alzheimer's disease via inhibiting of JNK signaling pathway, Phytomedicine 112 (2023), 154714, https://doi.org/10.1016/j.phymed.2023.154714.

[5] S.N. Rai, C. Singh, A. Singh, M.P. Singh, B.K. Singh, Mitochondrial dysfunction: a potential therapeutic target to treat Alzheimer's disease, Mol. Neurobiol. 57 (2020) 3075–3088, https://doi.org/10.1007/s12035-020-01945-y.

[6] P. Srivastava, P.N. Tripathi, P. Sharma, S.N. Rai, S.P. Singh, R.K. Srivastava, S. Shankar, S.K. Shrivastava, Design and development of some phenyl benzoxazole derivatives as a potent acetylcholinesterase inhibitor with antioxidant property to enhance learning and memory, Eur. J. Med. Chem. 163 (2019) 116–135, https://doi.org/10.1016/j.ejmech.2018.11.049.

[7] I. Gameiro, P. Michalska, G. Tenti, Á. Cores, I. Buendia, A.I. Rojo, N. D. Georgakopoulos, J.M. Hernández-Guijo, M. Teresa Ramos, G. Wells, M.G. López, A. Cuadrado, J.C. Menéndez, R. León, Discovery of the first dual GSK3β inhibitor/Nrf2 inducer. A new multitarget therapeutic strategy for Alzheimer's disease, Sci. Rep. 7 (2017), 45701, https://doi.org/10.1038/srep45701.

[8] G.R. Steinberg, D.G. Hardie, New insights into activation and function of the AMPK, Nat. Rev. Mol. Cell Biol. 24 (2023) 255–272, https://doi.org/10.1038/s41580-022-00547-x.

[9] Y. Ge, M. Zhou, C. Chen, X. Wu, X. Wang, Role of AMPK mediated pathways in autophagy and aging, Biochimie 195 (2022) 100–113, https://doi.org/10.1016/j.biochi.2021.11.008.

[10] T. Suzuki, D. Bridges, D. Nakada, G. Skiniotis, S.J. Morrison, J.D. Lin, A.R. Saltiel, K. Inoki, Inhibition of AMPK Catabolic Action by GSK3, Mol. Cell 50 (2013) 407–419, https://doi.org/10.1016/j.molcel.2013.03.022.

[11] Y. Zhang, N. Huang, F. Yan, H. Jin, S. Zhou, J. Shi, F. Jin, Diabetes mellitus and Alzheimer's disease: GSK-3β as a potential link, Behav. Brain Res. 339 (2018) 57–65, https://doi.org/10.1016/j.bbr.2017.11.015.

[12] A. Osama, J. Zhang, J. Yao, X. Yao, J. Fang, Nrf2: a dark horse in Alzheimer's disease treatment, Ageing Res. Rev. 64 (2020), 101206, https://doi.org/10.1016/j.arr.2020.101206.

[13] J. Cummings, Y. Zhou, G. Lee, K. Zhong, J. Fonseca, F. Cheng, Alzheimer's disease drug development pipeline: 2023, Alzheimers Dement. 9 (2023), e12385, https://doi.org/10.1002/trc2.12385.

[14] S.N. Pandey, N.K. Rangra, S. Singh, S. Arora, V. Gupta, Evolving role of natural products from traditional medicinal herbs in the treatment of Alzheimer's disease, ACS Chem. Neurosci. 12 (2021) 2718–2728, https://doi.org/10.1021/acschemneuro.1c00206.

[15] A.S. Gehren, W.F. De Souza, A.C.M. Sousa-Squiavinato, D.A.A. Ramos, B.R.B. Pires, E.S.F.W. Abdelhay, J.A. Morgado-Diaz, Parthenolide inhibits proliferation and invasion, promotes apoptosis, and reverts the cell–cell adhesion loss through downregulation of NF-κB pathway TNF-α-activated in colorectal cancer cells, Cell Biol. Int. (2023), cbin.12060, https://doi.org/10.1002/cbin.12060.

[16] R.R.A. Freund, P. Gobrecht, D. Fischer, H.-D. Arndt, Advances in chemistry and bioactivity of parthenolide, Nat. Prod. Rep. 37 (2020) 541–565, https://doi.org/10.1039/C9NP00049F.

[17] L. Liu, L. Feng, J. Gao, J. Hu, A. Li, Y. Zhu, C. Zhang, B. Qiu, Z. Shen, Parthenolide targets NLRP3 to treat inflammasome-related diseases, Int. Immunopharmacol. 119 (2023), 110229, https://doi.org/10.1016/j.intimp.2023.110229.

[18] Y. Zhang, L. Miao, Q. Peng, X. Fan, W. Song, B. Yang, P. Zhang, G. Liu, J. Liu, Parthenolide modulates cerebral ischemia-induced microglial polarization and alleviates neuroinflammatory injury via the RhoA/ROCK pathway, Phytomedicine 105 (2022), 154373, https://doi.org/10.1016/j.phymed.2022.154373.

[19] A. Perelman, C. Wachtel, M. Cohen, S. Haupt, H. Shapiro, A. Tzur, JC-1: alternative excitation wavelengths facilitate mitochondrial membrane potential cytometry, Cell Death Dis. 3 (2012), e430–e430, https://doi.org/10.1038/cddis.2012.171.

[20] O.G. Lyublinskaya, Ju.S. Ivanova, N.A. Pugovkina, I.V. Kozhukharova, Z. V. Kovaleva, A.N. Shatrova, N.D. Aksenov, V.V. Zenin, Yu.A. Kaulin, I.A. Gamaley, N.N. Nikolsky, Redox environment in stem and differentiated cells: a quantitative approach, Redox Biol. 12 (2017) 758–769, https://doi.org/10.1016/j.redox.2017.04.016.

[21] T. Gaojian, Q. Dingfei, L. Linwei, W. Xiaowei, Z. Zheng, L. Wei, Z. Tong, N. Benxiang, Q. Yanning, Z. Wei, C. Jian, Parthenolide promotes the repair of spinal cord injury by modulating M1/M2 polarization via the NF-κB and STAT 1/3 signaling pathway, Cell Death Discov. 6 (2020), 97, https://doi.org/10.1038/s41420-020-00333-8.

[22] M.Z. Othman, Z. Hassan, A.T. Che Has, Morris water maze: a versatile and pertinent tool for assessing spatial learning and memory, Exp. Anim. 71 (2022) 264–280, https://doi.org/10.1538/expanim.21-0120.

[23] L. She, L. Xiong, L. Li, J. Zhang, J. Sun, H. Wu, J. Ren, W. Wang, X. Zhao, G. Liang, Ginsenoside Rk3 ameliorates Aβ-induced neurotoxicity in APP/PS1 model mice via AMPK signaling pathway, Biomed. Pharmacother. 158 (2023), 114192, https://doi.org/10.1016/j.biopha.2022.114192.

[24] J.F. Oliveira Da Cruz, M. Gomis-Gonzalez, R. Maldonado, G. Marsicano, A. Ozaita, A. Busquets-Garcia, An alternative maze to assess novel object recognition in mice, Bio Protoc. 10 (2020), https://doi.org/10.21769/BioProtoc.3651.

[25] S. Ciudad, E. Puig, T. Botzanowski, M. Meigooni, A.S. Arango, J. Do, M. Mayzel, M. Bayoumi, S. Chaignepain, G. Maglia, S. Cianferani, V. Orekhov, E. Tajkhorshid, B. Bardiaux, N. Carulla, Aβ(1-42) tetramer and octamer structures reveal edge conductivity pores as a mechanism for membrane damage, Nat. Commun. 11 (2020), 3014, https://doi.org/10.1038/s41467-020-16566-1.

[26] J. Wang, M. Tong, B. Zhao, G. Zhu, D. Xi, J. Yang, Parthenolide ameliorates intracerebral hemorrhage-induced brain injury in rats, Phytother. Res. 34 (2020) 153–160, https://doi.org/10.1002/ptr.6510.

[27] C. Rummel, R. Gerstberger, J. Roth, T. Hübschle, Parthenolide attenuates LPS-induced fever, circulating cytokines and markers of brain inflammation in rats, Cytokine 56 (2011) 739–748, https://doi.org/10.1016/j.cyto.2011.09.022.

[28] K. Kanninen, T.M. Malm, H.-K. Jyrkkänen, G. Goldsteins, V. Keksa-Goldsteine, H. Tanila, M. Yamamoto, S. Ylä-Herttuala, A.-L. Levonen, J. Koistinaho, Nuclear factor erythroid 2-related factor 2 protects against beta amyloid, Mol. Cell Neurosci. 39 (2008) 302–313, https://doi.org/10.1016/j.mcn.2008.07.010.
[29] L.M. Billings, S. Oddo, K.N. Green, J.L. McGaugh, F.M. LaFerla, Intraneuronal Aβ causes the onset of early Alzheimer's disease-related cognitive deficits in transgenic mice, Neuron 45 (2005) 675–688, https://doi.org/10.1016/j.neuron.2005.01.040.
[30] J. Doroszkiewicz, B. Mroczko, New possibilities in the therapeutic approach to Alzheimer's disease, Int. J. Mol. Sci. 23 (2022) 8902, https://doi.org/10.3390/ijms23168902.
[31] A.B. Reiss, D. Muhieddine, B. Jacob, M. Mesbah, A. Pinkhasov, I.H. Gomolin, M. M. Stecker, T. Wisniewski, J. De Leon, Alzheimer's disease treatment: the search for a breakthrough, Medicina 59 (2023) 1084, https://doi.org/10.3390/medicina59061084.
[32] W. Wuli, S.T. Tsai, T.W. Chiou, H.J. Harn, Human-induced pluripotent stem cells and herbal small-molecule drugs for treatment of Alzheimer's disease, Int. J. Mol. Sci. 21 (2020) 1327, https://doi.org/10.3390/ijms21041327.
[33] Z. Zhang, K. Zhang, M. Zhang, X. Zhang, R. Zhang, Parthenolide suppresses T helper 17 and alleviates experimental autoimmune encephalomyelitis, Front. Immunol. 13 (2022), 856694, https://doi.org/10.3389/fimmu.2022.856694.
[34] F. Fagiani, C. Lanni, M. Racchi, S. Govoni, Targeting dementias through cancer kinases inhibition, Alzheimers Dement. 6 (2020), e12044, https://doi.org/10.1002/trc2.12044.
[35] H. Nakabayashi, K. Shimizu, Involvement of Akt/NF-κB pathway in antitumor effects of parthenolide on glioblastoma cells in vitro and in vivo, BMC Cancer 12 (2012), 453, https://doi.org/10.1186/1471-2407-12-453.
[36] S.N. Rai, W. Zahra, H. Birla, S.S. Singh, S.P. Singh, Commentary: mild endoplasmic reticulum stress ameliorates lpopolysaccharide-induced neuroinflammation and cognitive impairment via regulation of microglial polarization, Front. Aging Neurosci. 10 (2018), 192, https://doi.org/10.3389/fnagi.2018.00192.
[37] L. Cai, Q. Gong, L. Qi, T. Xu, Q. Suo, X. Li, W. Wang, Y. Jing, D. Yang, Z. Xu, F. Yuan, Y. Tang, G. Yang, J. Ding, H. Chen, H. Tian, ACT001 attenuates microglia-mediated neuroinflammation after traumatic brain injury via inhibiting AKT/NFκB/NLRP3 pathway, Cell Commun. Signal. 20 (2022), 56, https://doi.org/10.1186/s12964-022-00862-y.
[38] P.N. Tripathi, P. Srivastava, P. Sharma, M.K. Tripathi, A. Seth, A. Tripathi, S.N. Rai, S.P. Singh, S.K. Shrivastava, Biphenyl-3-oxo-1,2,4-triazine linked piperazine derivatives as potential cholinesterase inhibitors with anti-oxidant property to improve the learning and memory, Bioorg. Chem. 85 (2019) 82–96, https://doi.org/10.1016/j.bioorg.2018.12.017.
[39] R.S. Albalawi, L.S. Binmahfouz, R.H. Hareeri, R.A. Shaik, A.M. Bagher, Parthenolide phytosomes attenuated gentamicin-induced nephrotoxicity in rats via activation of Sirt-1, Nrf2, OH-1, and NQO1 axis, Molecules 28 (2023) 2741, https://doi.org/10.3390/molecules28062741.
[40] K. Ono, T. Hamaguchi, H. Naiki, M. Yamada, Anti-amyloidogenic effects of antioxidants: implications for the prevention and therapeutics of Alzheimer's disease, Biochim. Biophys. Acta 1762 (2006) 575–586, https://doi.org/10.1016/j.bbadis.2006.03.002.
[41] J. Duan, J. Cui, Z. Yang, C. Guo, J. Cao, M. Xi, Y. Weng, Y. Yin, Y. Wang, G. Wei, B. Qiao, A. Wen, Neuroprotective effect of Apelin 13 on ischemic stroke by activating AMPK/GSK-3β/Nrf2 signaling, J. Neuroinflamm. 16 (2019), 24, https://doi.org/10.1186/s12974-019-1406-7.
[42] K.A. DiTacchio, S.F. Heinemann, G. Dziewczapolski, Metformin treatment alters memory function in a mouse model of Alzheimer's disease, J. Alzheimers Dis. 44 (2015) 43–48, https://doi.org/10.3233/JAD-141332.
[43] S. Li, X. Zhao, P. Lazarovici, W. Zheng, Artemether activation of AMPK/GSK3β (ser9)/Nrf2 signaling confers neuroprotection towards β-amyloid-induced neurotoxicity in 3×Tg Alzheimer's mouse model, Oxid. Med. Cell. Longev. 2019 (2019) 1–24, https://doi.org/10.1155/2019/1862437.
[44] A.J.T. Yang, A. Bagit, R.E.K. MacPherson, Resveratrol, metabolic dysregulation, and Alzheimer's disease: considerations for neurogenerative disease, Int. J. Mol. Sci. 22 (2021) 4628, https://doi.org/10.3390/ijms22094628.